

Redshift dependent cosmic birefringence from axion-like dark matter

Matteo Galaverni^{a,b,*}

^a*Specola Vaticana (Vatican Observatory),
V-00120, Vatican City State*

^b*INAF/OAS Bologna,
via Gobetti 101, I-40129 Bologna, Italy*

E-mail: matteo.galaverni@gmail.com

We highlight the importance of taking into account the redshift evolution of cosmic birefringence (rotation of linear polarization angle) in order to evaluate CMB polarization power spectra. Focusing particularly on isotropic birefringence from axion-like dark matter we discuss the limits on axion-photon coupling constant.

*41st International Conference on High Energy physics - ICHEP2022
6-13 July, 2022
Bologna, Italy*

*Speaker

1. Introduction - redshift dependent isotropic birefringence

One of the most studied interactions in order to look for pseudoscalar particles ϕ is their coupling with photons:

$$-\frac{g_\phi}{4}\phi F_{\mu\nu}\tilde{F}^{\mu\nu}, \quad (1)$$

where g_ϕ is the photon-axion coupling constant and $\tilde{F}^{\mu\nu}$ is the dual of the electromagnetic tensor $F_{\mu\nu}$. Several limits on this coupling constant are present in literature both from laboratory experiments (photon polarization, light shining through walls, microwave cavity, ...) and astrophysical observations (stellar energy-loss limits, conversion of astrophysical axion fluxes in magnetic fields, axion helioscopes, ...); see [1] and references therein for more details.

When a photon propagates in an evolving pseudoscalar field background it experiences a rotation of the linear polarization plane (cosmic birefringence) [2, 3]. In this work we focus on the isotropic and frequency independent rotation, therefore the effect is fully characterized by an angle $\alpha(\eta)$, where η is the conformal time¹:

$$\alpha(\eta) = \frac{g_\phi}{2} \int_{\eta_{\text{em}}}^{\eta} \phi'(\eta_1) d\eta_1, \quad (2)$$

here η_{em} is time at emission and ϕ' is the derivative with respect conformal time. Cosmic Microwave Background (CMB) polarization is a very good probe to study this effect on cosmological timescales.

In this work we do not consider only the total variation of the linear polarization angle, but we also take into account its *time/redshift dependence* during propagation along the line-of-sight. We study the Boltzmann equation for the linear polarization Stokes parameters Q and U with an additional term (second line) due to isotropic birefringence [5–7]:

$$\begin{aligned} \Delta'_{Q\pm iU}(k, \eta) + ik\mu\Delta_{Q\pm iU}(k, \eta) &= -n_e\sigma_T a(\eta) \left[\Delta_{Q\pm iU}(k, \eta) + \sum_m \sqrt{\frac{6\pi}{5}} {}_{\pm 2}Y_2^m S_P^{(m)}(k, \eta) \right] \\ &\mp i2\alpha'(\eta)\Delta_{Q\pm iU}(k, \eta). \end{aligned} \quad (3)$$

The cosine of the angle between the CMB photon direction and the Fourier wave vector is indicated by μ , n_e is the number density of free electrons, σ_T is the Thomson cross section, ${}_sY_2^m$ are spherical harmonics with spin-weight s , $S_P^{(m)}(k, \eta)$ is the source term generating linear polarization, and $\alpha'(\eta)$ is the derivative of the rotation angle with respect conformal time. In order to consider also the effects due redshift/time dependence of the birefringence angle we numerically solve Eq. (3) using a modified version of the Boltzmann code CAMB [8].

Isotropic birefringence is frequently described considering only the *total variation of the linear polarization angle* during propagation from recombination (rec) to today. Under this assumption polarization power spectra are modified following these relations [7, 9–12]:

$$\begin{aligned} C_\ell^{TE, \text{const}} &= C_\ell^{TE, \text{rec}} \cos(2\bar{\alpha}), \quad C_\ell^{EE, \text{const}} = C_\ell^{EE, \text{rec}} \cos^2(2\bar{\alpha}), \quad C_\ell^{BB, \text{const}} = C_\ell^{EE, \text{rec}} \sin^2(2\bar{\alpha}), \\ C_\ell^{TB, \text{const}} &= C_\ell^{TE, \text{rec}} \sin(2\bar{\alpha}), \quad C_\ell^{EB, \text{const}} = \frac{1}{2} C_\ell^{EE, \text{rec}} \sin(4\bar{\alpha}), \end{aligned} \quad (4)$$

¹We use natural units, $\hbar = c = 1$, and assume flat Λ CDM cosmological model with *Planck* 2018 estimates of cosmological parameters [4]: $\Omega_b h^2 = 0.02237$, $\Omega_c h^2 = 0.120$, $\tau = 0.0544$, $n_s = 0.9649$, $\ln(10^{10} A_s) = 3.044$, $H_0 = 100 h \text{ km s}^{-1} \text{ Mpc}^{-1} = 67.36 \text{ km s}^{-1} \text{ Mpc}^{-1}$.

here $\bar{\alpha} \equiv \alpha(\eta_{\text{rec}}) - \alpha(\eta_0)$ is the total rotation of the linear polarization angle between recombination and today; we have assumed no odd power spectra at recombination ($C_\ell^{TB,\text{rec}} = C_\ell^{EB,\text{rec}} = 0$) and $C_\ell^{BB,\text{rec}} = 0$.

In Fig. 1 we consider different phenomenological time dependencies of the birefringence angle, with the same total variation $\bar{\alpha}$. According to the widely used approximation of Eqs. (4)-(5) we should obtain the same power spectra, but using the modified version of CAMB based on Eq. (3) we clearly see that different time evolution profiles induce different multipole dependencies of the power spectra [5, 6, 13–15].

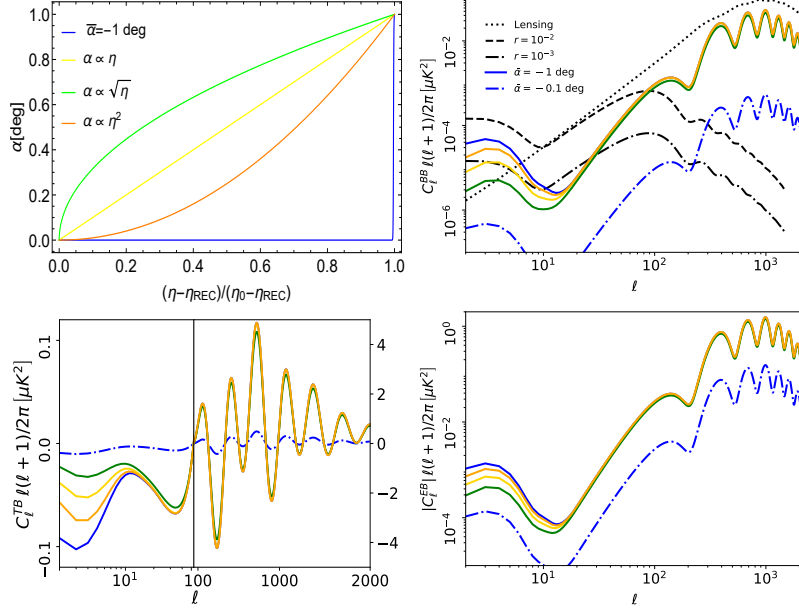


Figure 1: (a) Evolution of the birefringence angle as a function of conformal time $(\eta - \eta_{\text{rec}}) / (\eta_0 - \eta_{\text{rec}})$: in all four phenomenological cases α starts from $\alpha(\eta_{\text{rec}}) = 0$ deg and arrives at $\alpha(\eta_{\text{rec}}) = 1$ deg, the green line corresponds to a growth proportional to $\sqrt{\eta}$, the yellow line to a linear growth, the orange line to a growth proportional to η^2 , and the blue continuous line to a detector miscalibration of -1 deg; (b) C_ℓ^{BB} obtained using the approximation of Eqs. (4)-(5) for $\bar{\alpha} = -1$ deg ($\bar{\alpha} = -0.1$ deg) blue continuous (dash-dotted) line, and the modified version of CAMB (green, yellow, and orange line); we plot for comparison also the signal induced by gravitational lensing (black dotted line), primordial signal for a tensor to scalar ratio $r = 10^{-2}$ (black dashed line), and $r = 10^{-3}$ (black dot-dashed line); (c) C_ℓ^{TB} ; (d) C_ℓ^{EB} .

2. Cosmic birefringence for axion-like dark matter

Review of Particle Physics [1] reports now also a limit on g_ϕ obtained from CMB birefringence [16]:

$$|g_\phi| \lesssim 9.6 \times 10^{-14} \text{ GeV}^{-1}, \quad (6)$$

for an axion like particle of mass $m = 10^{-22}$ eV, using existing *Planck* results [4] and neglecting the details of the redshift evolution of the axion field along the line-of-sight.

Assuming that the pseudoscalar particles contribute to dark matter density, we reconstruct the evolution of the field as a function of time $\phi(\eta)$, see [6]. The evolution of the birefringence angle is obtained using Eq. (2). We solve numerically the modified Boltzmann Eq. (3) and obtain the

rotated CMB power spectra taking into account also the time dependence of the linear polarization angle, see Fig. 2 for C_ℓ^{BB} .

Recent analyses of *Planck* data combined with *WMAP* 9-year data provide hints of isotropic cosmic birefringence with $\bar{\alpha} = 0.342_{-0.091}^{+0.094}$ deg [17]. If we want obtain a rotation of this order of magnitude with our modified version of CAMB we have to consider a coupling constant:

$$g_\phi \sim 1.5 \times 10^{-14} \text{ GeV}^{-1}, \quad (7)$$

always assuming $m = 10^{-22}$ eV. See Fig. 2 for C_ℓ^{BB} induced by a coupling of this order of magnitude.

If we want to obtain the same birefringence for heavier masses ($m = 10^{-20}$ eV), we have to consider a bigger coupling constant $g_\phi \sim 8.0 \times 10^{-13} \text{ GeV}^{-1}$; on the contrary for lighter masses ($m = 10^{-24}$ eV), the coupling constant is smaller $g_\phi \sim 2.3 \times 10^{-16} \text{ GeV}^{-1}$. In Fig. 3 we plot C_ℓ^{BB} obtained by the modified version of CAMB for the values considered above, and compare them with the C_ℓ^{BB} obtained by Eq. (4) assuming $\bar{\alpha} = 0.34$ deg. For a detailed χ^2 comparison of the polarization power spectra we refer to [18].

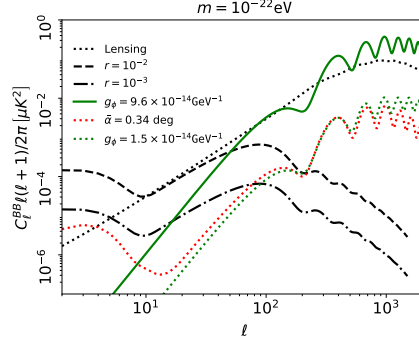


Figure 2: Axion-like dark matter: C_ℓ^{BB} with time dependent isotropic cosmic birefringence fixed $m = 10^{-22}$ eV and $g_\phi = 9.6 \times 10^{-14} \text{ GeV}^{-1}$ ($g_\phi = 1.5 \times 10^{-14} \text{ GeV}^{-1}$) green continuous (dotted) line; we plot for comparison also the power spectra obtained using Eq. (4) for $\bar{\alpha} = 0.34$ deg (red dotted line); the signal induced by gravitational lensing (black dotted line), primordial signal for $r = 10^{-2}$ (black dashed line), and $r = 10^{-3}$ (black dot-dashed line).

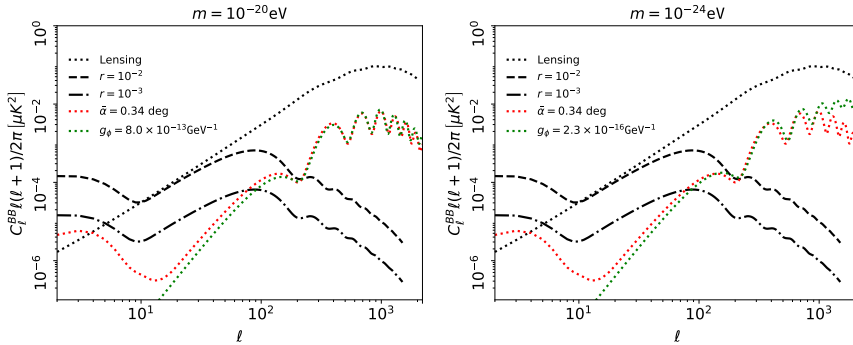


Figure 3: (a) Axion-like dark matter: C_ℓ^{BB} with time dependent isotropic cosmic birefringence fixed $m = 10^{-20}$ eV and $g_\phi = 8.0 \times 10^{-13} \text{ GeV}^{-1}$, we plot for comparison also the power spectra obtained using Eq. (4) for $\bar{\alpha} = 0.34$ deg (red dotted line); the signal induced by gravitational lensing (black dotted line), primordial signal for $r = 10^{-2}$ (black dashed line), and $r = 10^{-3}$ (black dot-dashed line); (b) same plot for lighter mass ($m = 10^{-24}$ eV) fixed $g_\phi = 2.3 \times 10^{-16} \text{ GeV}^{-1}$.

3. Conclusions - limits on axion-photon coupling

We highlighted the importance of taking into account the time/redshift evolution of the birefringence angle in order to evaluate CMB polarization power spectra. We discussed first the phenomenological case of birefringence angles varying from 0 to 1 deg with different time dependencies and showed the effects on the power spectra. Later, in Section. 2, we considered a pseudoscalar acting as dark matter. In Fig. 4 we compared the limits on the axion-photon coupling obtained from isotropic cosmic birefringence with the other limits present in literature [1, 19]. CMB cosmic birefringence nicely complements other experimental/astrophysical tests. We provided here a qualitative description of the importance of taking into account time/redshift evolution of the birefringence angle and we refer to [18] for a more detailed discussion.

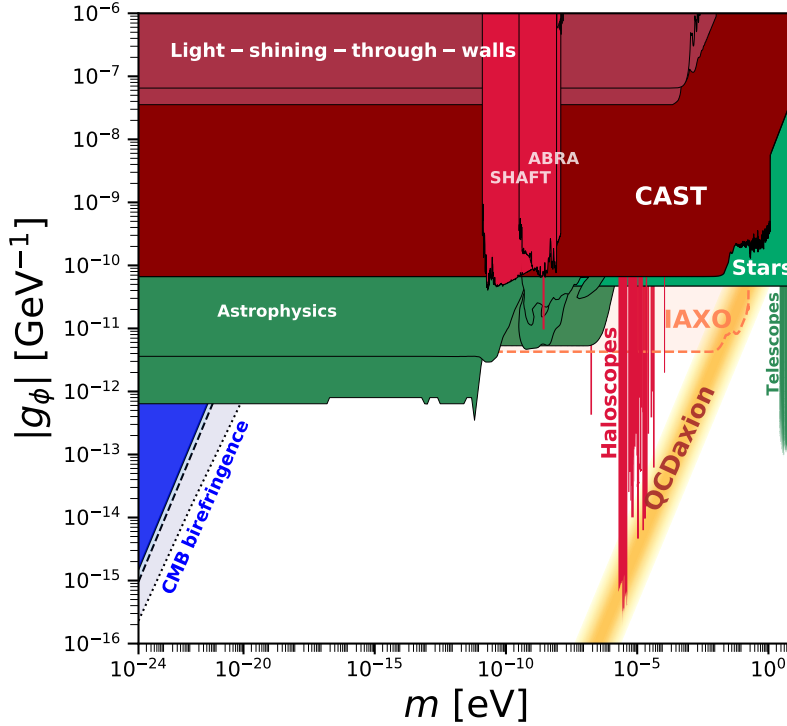


Figure 4: Limits for the axion-photon coupling constant g_ϕ as a function of mass m (coloured regions are excluded). Dark blue region corresponds to CMB birefringence limits presented in [6], blue dashed line corresponds to CMB birefringence limits discussed in [16], light blue dotted line corresponds to CMB birefringence of the order of 0.34 deg [17] taking into account the redshift dependency of the birefringence angle, as discussed here in Section 2. Plot created with the `AxionLimits` code [19], we refer to online documentation for references on the other constraints.

References

- [1] R. L. Workman *et al.* [Particle Data Group], “Review of Particle Physics,” *PTEP* **2022**, 083C01 (2022) doi:10.1093/ptep/ptac097
- [2] S. M. Carroll, G. B. Field and R. Jackiw, *Phys. Rev. D* **41**, 1231 (1990) doi:10.1103/PhysRevD.41.1231

- [3] D. Harari and P. Sikivie, *Phys. Lett. B* **289** (1992) 67.
- [4] N. Aghanim *et al.* [Planck], *Astron. Astrophys.* **641**, A6 (2020) [erratum: *Astron. Astrophys.* **652**, C4 (2021)] doi:10.1051/0004-6361/201833910 [arXiv:1807.06209 [astro-ph.CO]].
- [5] G. C. Liu, S. Lee and K. W. Ng, *Phys. Rev. Lett.* **97**, 161303 (2006) doi:10.1103/PhysRevLett.97.161303 [arXiv:astro-ph/0606248 [astro-ph]].
- [6] F. Finelli and M. Galaverni, *Phys. Rev. D* **79** (2009), 063002 doi:10.1103/PhysRevD.79.063002 [arXiv:0802.4210 [astro-ph]].
- [7] G. Gubitosi, M. Martinelli and L. Pagano, *JCAP* **12**, 020 (2014) doi:10.1088/1475-7516/2014/12/020 [arXiv:1410.1799 [astro-ph.CO]].
- [8] A. Lewis, A. Challinor and A. Lasenby, *Astrophys. J.* **538**, 473-476 (2000) doi:10.1086/309179 [arXiv:astro-ph/9911177 [astro-ph]].
- [9] A. Lue, L. M. Wang and M. Kamionkowski, *Phys. Rev. Lett.* **83**, 1506-1509 (1999) doi:10.1103/PhysRevLett.83.1506 [arXiv:astro-ph/9812088 [astro-ph]].
- [10] B. Feng, H. Li, M. z. Li and X. m. Zhang, *Phys. Lett. B* **620**, 27-32 (2005) doi:10.1016/j.physletb.2005.06.009 [arXiv:hep-ph/0406269 [hep-ph]].
- [11] A. Gruppuso, G. Maggio, D. Molinari and P. Natoli, *JCAP* **05**, 020 (2016) doi:10.1088/1475-7516/2016/05/020 [arXiv:1604.05202 [astro-ph.CO]].
- [12] Y. Minami, H. Ochi, K. Ichiki, N. Katayama, E. Komatsu and T. Matsumura, *PTEP* **2019**, no.8, 083E02 (2019) doi:10.1093/ptep/ptz079 [arXiv:1904.12440 [astro-ph.CO]].
- [13] M. Galaverni, *Astrophys. Space Sci. Proc.* **51**, 165-174 (2018) doi:10.1007/978-3-319-67205-2_11
- [14] B. D. Sherwin and T. Namikawa, [arXiv:2108.09287 [astro-ph.CO]].
- [15] H. Nakatsuka, T. Namikawa and E. Komatsu, *Phys. Rev. D* **105**, no.12, 123509 (2022) doi:10.1103/PhysRevD.105.123509 [arXiv:2203.08560 [astro-ph.CO]].
- [16] M. A. Fedderke, P. W. Graham and S. Rajendran, *Phys. Rev. D* **100**, no.1, 015040 (2019) doi:10.1103/PhysRevD.100.015040 [arXiv:1903.02666 [astro-ph.CO]].
- [17] J. R. Eskilt and E. Komatsu, *Phys. Rev. D* **106**, no.6, 063503 (2022) doi:10.1103/PhysRevD.106.063503 [arXiv:2205.13962 [astro-ph.CO]].
- [18] M. Galaverni, F. Finelli and D. Paoletti, in preparation (2022).
- [19] C. O'Hare, Zenodo (2020), <https://cajohare.github.io/AxionLimits/> doi:10.5281/zenodo.3932430.